*Paper*

# Modified PSO Based Channel Allocation Scheme for Interference Management in 5G Wireless Mesh Networks

Nirmalkumar S. Benni and Sunilkumar S. Manvi

*Department of Electronics and Communication Engineering, REVA Institute of Technology and Management, Bangalore, Karnataka, India*

https://doi.org/10.26636/jtit.2022.156621

**Abstract—Efficient channel management is a challenge that next-generation wireless networks need to meet in order to satisfy increasing bandwidth demand and transmission rate requirements. Non-orthogonal multiple access (NOMA) is one of such efficient channel allocation methods used in 5G backhaul wireless mesh networks. In this paper, we propose a power demand-based channel allocation method for 5G backhaul wireless mesh networks by employing NOMA and considering traffic demands in small cells, thereby improving channel utility. In this scheme, we work with physical layer transmission. The foremost aim is to mutually optimize the uplink/downlink NOMA channel assignment in order to increase user fairness. The approach concerned may be divided into two steps. First, initial channel allocation is performed by employing the traveling salesman problem (TSP), due to its similarity to many-to-many double-side user-channel allocation. Second, the modified particle swarm optimization (PSO) method is applied for allocation updates, by introducing a decreasing coefficient which may have the form of a standard stochastic estimate algorithm. To enhance exploration capacity of modified the PSO, a random velocity is included to optimize the convergence rate and exploration behavior. The performance of the designed scheme is estimated through simulation, taking into account such parameters as throughput, spectral efficiency, sum-rate, outage probability, signal-to-interference plus noise ratio (SINR), and fairness. The proposed scheme maximizes network capacity and improves fairness between the individual stations. Experimental results show that the proposed technique performs better than existing solutions.**

***Keywords—channel allocation, co-channel interference, convex optimization, multicarrier NOMA, Rayleigh fading.***

## 1. Introduction

5G is a trending communication technology that is capable of improving network performance in urban areas [1]. 5G enhances the collection of information and the framework measurement rate. The data transmission rate, thickness association, and inactivity of ultra-low signals are the other benefits of 5G development enjoyed in multiple input multiple output (MIMO) systems.

Association of the web with remote cell towers is known as the concept of backhaul. In multi-level media communication, the backhaul region consists of a system characterized by a specific orientation of its connections, e.g. spine organization, center system, and the edge of the progressive area [2]. Backhaul improves the speed at which information is exchanged. Genuinely, without backhaul, users would not be able to enjoy a web relationship in any way, shape or form. Therefore, the backhaul effect should be considered to provide a high priority information background.

Prerequisites of this type affect backhaul in a peculiar manner, as it may bear information with highly complex and flexible green contemplation [3]. These effects are very difficult to acknowledge and secure 5G communication-based protocols in the networking environment. Media communications organization handles expansive volume spilling information and uphold experiences from peculiarity recognition and prescient displaying to comprehend their systems and their clients [4], [5]. In this way, the presumption of security segment of existing cell frameworks, which rely upon making sure about the significant attainable quality and guard of end-users, the 5G cell structure is depended upon to ensure that a redesigned security instrument is set up in general framework to address issues of approval and support for various interconnected IoT devices.

Many methods are available for enhancing the uplink stream. Versatile quality of service (QoS)-related environments may affect the system of 5G communication-based portable hubs in terms of their collection ability [6], [7]. NOMA is a prominent access system for executing upgrades in cutting-edge cell interchanges. Contrasted with symmetrical recurrence division different access, which is a notable high-limit orthogonal multiple access scheme, NOMA offers a range of tempting advantages, including higher pro-

ductivity. A variety of NOMA strategies exist, including power-area and code-domain [8].
The diverse and demanding characteristics of 5G require a move from the rigid systems of the past, towards more flexible and versatile networks. The use of recently developed radio network technologies results in an improvement of dimensional flexibility in 5G networks [9]. New handoff solutions are likewise encouraging in the Internet of Things (IoT) applications [10]. As we gain ground about the 5G network of remote systems, the bit-per-joule energy efficiency turns into an imperative structure paradigm for practical advancement [11]. With that considered, MIMO-related innovations turn out to be one of the major empowering agents for 5G solutions in which BSs are furnished with adequate reception hardware to satisfy requirements related to phantom and energy efficiency increases over current LTE systems [12].

### *1.1. Problem Statement*

5G wireless networks are expected to support very diverse applications and terminals. Massive connectivity with a large number of devices is an important requirement. In the 5G era, the evolution of heterogeneous networks (Het-Nets) results in densification of different sizes of cells. Due to the time- and space-dependent service requirements and traffic patterns, time-varying asymmetric traffic loads are expected in both uplink (UL) and downlink (DL) connections in different cells. Many optimization strategies have been designed to provide seamless coverage and QoS in DL and UL. However, the intractable nature of the channel selection problem motivates us to design an efficient channel allocation scheme through joint optimization of UL and DL streams. Performance of the designed scheme is estimated through Matlab, with such performance parameters as throughput, spectral efficiency, sum-rate, outage probability, signal-to-interference plus noise ratio (SINR) and fairness taken into consideration and compared with other recent optimization techniques.

### *1.2. Research Contributions*

In this paper, we examine a 5G wireless mesh network that comprises multiple primary networks and subscribed users (SUs). At any instant, a different number of channels with different capacities is allocated by the primary networks to each SU.
The channel allocation problem is formulated as TSP, which is then associated with the many-to-many two-sided user-channel allocation. We acquaint a diminishing coefficient with the updating principle. Thus, the population-based artificial intelligence (AI) concept is used in our work, i.e. a modified PSO may be perceived as a standard stochastic estimate algorithm.
The modified PSO is then used to jointly optimize both uplink and downlink channels using NOMA for optimal channel allocation with proper interference management.
Finally, we mutually reform the UL/DL channel allocation using NOMA to widen user fairness with proper interference management.
The related works are discussed in Section 2. Section 3 describes the system model. Section 4 elaborates on the proposed method. Section 5 evaluates performance of the channel allocation process. Section 6 presents the conclusions.

## 2. Related Works

Xia *et al*. [13] proposed a new kind of virtual channel optimization technique in NOMA for successful power balancing. By using the process presented, data may be separated through the power balancing effect. The minimum Euclidean distance for constellation points without estimating the channel is considered as the best method for the channel state estimation process. A closed-form of the optimization process is developed by maximizing the fixed optimal solution with 2 to 3 users. Also, the less complex effect of the maximum likelihood detector reduces computational intricacy without influencing the implementation of quadrature phase shift keying (QPSK).
Paper [14] proposed a calculation for the UL of huge MIMO frameworks to isolate the joined gotten flag of all clients at the BS into autonomous signs for every client class. While applying the proposed calculation, the computational expense of the flag handling process is diminished and it is conceivable to ensure adaptability on the location methods at the BS. A flag is shown for heterogeneous systems with various classes of clients. Discretionary design cell acquisition subframes (CAS) and distributed antenna systems (DAS) are presented in this paper as well. Total rate examination and computational multifaceted nature contemplated for the proposed decoupled signal detection (DSD) method are exhibited.
In [15], user transmission rate and interference are mainly considered for developing a fractional transmission power allocation (FTPA)-based channel allocation process. Greedy algorithm (GA) is applied to obtain the ideal solution for allocation purposes. Mathematical development of max-min energy effectiveness is developed in the intractable programming solution. A sequential programming approach is determined to obtain an optimal solution for power analysis. Focus is placed on energy-efficient power-based channel allocation to provide an enhanced version of optimal channel modulation.
These upgrades demonstrate that a quality-of-service-aware game theory-based power control (QoS-GTPC) plan can be obtained for 5G versatile frameworks.
Sarigiannidis *et al*. [16] presented a spatially unique power control answer for relieving cell-to-device-to-device (D2D) and D2D-to-cell impedance. The proposed D2D control arrangement is somewhat adaptable, including the exceptional instances of no D2D connections or using the greatest transmit control. Under the considered power control, a diagnostic methodology is produced to assess the pro-

ductivity and proficiency of such systems. Investigation of the power control arrangement can productively alleviate obstruction between the cell and the D2D level.

In general, 5G wireless networks provide various facilities to assist assorted applications and terminals which require superb connectivity to connect an enormous number of devices. Han *et al*. [17] developed a security-related protocol for NOMA-based massive MIMO uplink communication. The power allocation model is given through the joint power and sub-channel allocation for secrecy capacity (JPSASC) method to get a sub-optimal solution to the joint issue. Especially, the power stint is developed as a non-pliable game with the perspective of a distribution system. The simulation outcome of JPSASC is developed to explain the secrecy capacity in the NOMA model.

5G networks can be configured as heterogeneous networks (HetNets), in which cell densification is the main feature, with cells of different sizes forming the network. Furthermore, 5G is relied upon to help alleviate time-shifting awry traffic load for both UL and DL connections in various cells. Several optimization strategies have been developed to support seamless coverage and QoS for both DL and UL. However, the intractable nature of the channel selection problem in 5G heterogeneous networks [18] motivates us to design an efficient channel allocation scheme through joint optimization of UL and DL streams.

## 3. System Model

Dense HetNets have been created based on the principle of diminishing the cell size and increasing the quantity of small cells (SCs) per unit of territory, as such a solution is capable of handling the traffic rates expected in 5G. Here, we consider a 5G heterogeneous network comprising $N$ networks of any type, e.g. wired and wireless links. The network consists of a specified number of primary users (PUs) and subscribed users (SUs). Each network is allocated with the most extreme number of channels, where the channels allocated to SUs rely on the conduct of PUs [19]. 5G supports a heterogeneous network that consists of discrete elements, such as users, services, radio access networks (RAN), and backhaul networks. The backhaul network plays a major role in transferring data intended for the users from/to different base stations within the cellular network. The scheduling of backhaul transmission determines that performance be optimized relative to traffic demands placed on the small cells served. Normally, the traffic demands may change over time during longer transmissions, due to channel dynamics.

We will probably meet long-duration traffic requests over blocks of $N$ diminishing slots. Next, the scheduling problem of more than one such block will be considered. On account of remote backhaul, the drawn-out requests will regularly be out of the ergodic rate locale of the backhaul remote channel. This persuades us to characterize the backhaul scheduling problem in order to decide on and work at the rate point in the backhaul ergodic rate area that is nearest, in some sense, to the traffic requests in the access network. An example of a 5G backhaul network and its components is depicted in Fig. 1.

With MIMO and millimeter-wave communication technologies, the small cell scheme is an inevitable solution for upcoming 5G networks. MIMO has arisen as an innovation catalyst for cutting edge mobile communications in 5G. Furthermore, the increase in channel allocation guaranteed by MIMO is forecast to overcome the capacity crunch experienced in current mobile networks and to allow for the

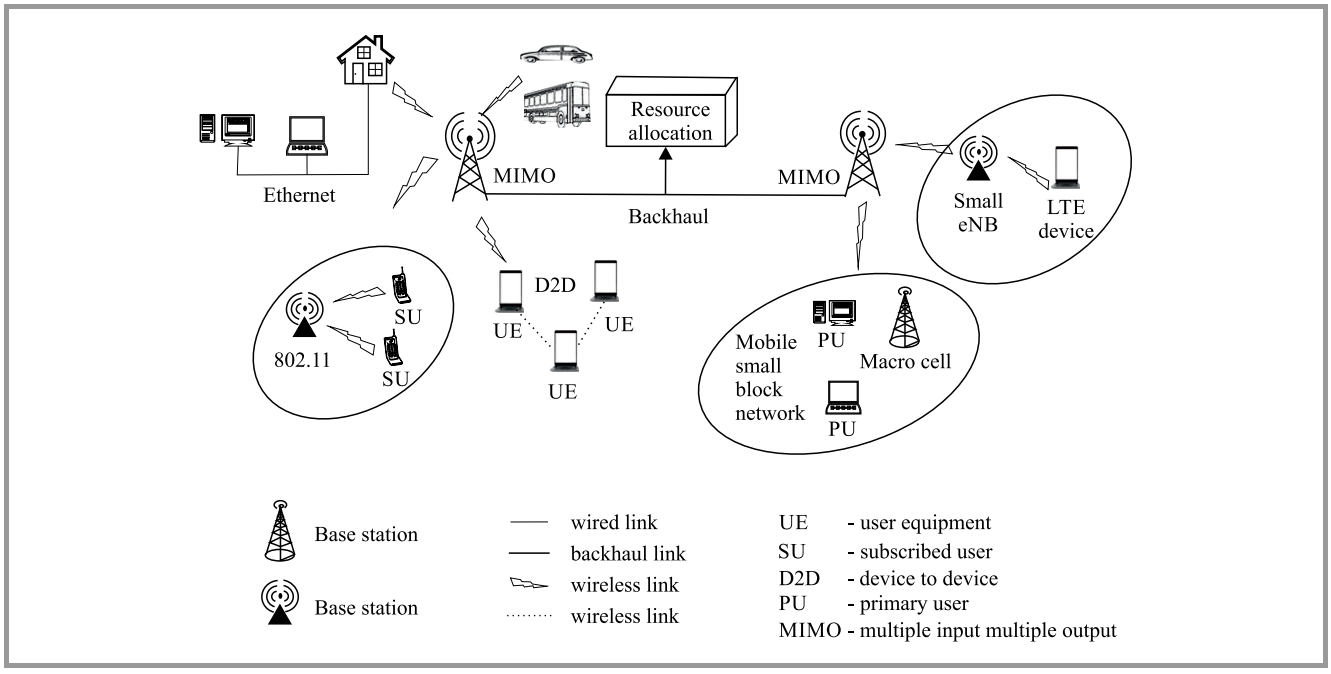


***Fig. 1.*** A 5G wireless mesh backhaul network.

aggressive focus of 5G. The test to acknowledge MIMO for 5G is an effective and cost-proficient reconciliation in the whole network concept. This work features categorization and usage schemes for MIMO with a small cell 5G indoor framework taken into consideration.
In this regard, the MIMO innovation, where the BSs are furnished with countless antennas to satisfy different spectral and energy efficiency gain requirements, will be a key innovation empowering agent for 5G [20], [21].

# 4. Proposed Method

We initially portray the basics of UL and DL NOMA transmissions and underline their vital differences in terms of usage unpredictability, recognition, and unraveling at the successive interference cancelation (SIC) receiver(s), brought about intra-cell and between cell impedance. At that point, for joint DL and UL NOMA, we hypothetically infer the NOMA predominant condition for every individual client in a two-client NOMA group. The NOMA predominant condition refers to a condition under which the spectral efficiency gains of NOMA are ensured, in contrast with orthogonal frequency division multiple access (OFDMA) [22]. By and large, NOMA permits the superposition of definite message signals of clients within a NOMA group. The ideal message signal is then recognized and decoded at the receiver (client in the DL and BS in the UL) by applying SIC.
Table 1 shows the notations used in the following considerations.

Table 1
Notations used

| Symbol | Description |
|---|---|
| $x_n$ | Unit power message signal for user $n$ |
| $p_n^d$ | Power allocated for user $n$ |
| $N$ | Total number of users |
| $Pt$ | Total power at base station |
| $w_n$ | Gaussian noise at the receiver for user $n$ |
| $h_n$ | Channel gain between the BS and user $n$ |
| $v_n$ | Additive noise |
| $v$ | Indicates the additive noise at the BS |
| $I_n$ | Interfering signal |
| $\theta$ | Power splitting factor |
| $w$ | Receiver noise |
| $R_n^u$ | Uplink rate achieved by the $n$-th user |
| $N_0$ | Noise power |
| $P_I$ | Power of the interference received by the base station |
| $\gamma_n^u$ | Uplink signal to noise ratio |
| $\gamma_n^d$ | Downlink signal to noise ratio |
| $P_m^i$ | Transmit power of downlink |
| $q_r^i$ | Transmit power of uplink |
| $\beta_m$ | Joint effect of path loss |
| $\beta_n$ | Shadowing between DL users and UL BSs |
| $x$ | Current number of iterations |
| $\alpha$, $\beta$ | Positive constant parameters |
| $a$ | Acceleration factor |
| $w$ | Inertia weight |
| $\phi$ | Path loss exponent |
| $\mu$ | Non-negative constant |
| $H, G$ | Constant parameters |

### *4.1. Downlink NOMA*

In the DL NOMA, the BS communicates the superimposed sign:

$$x = \sum_{n=1}^{N} \sqrt{P_n^d} x_n^d \ ,$$

where $x_n^d$ is the unit power of the message signal proposed for client $n$, $P_n^d$ means the power allocated for client $n$, and $N$ indicates the complete number of clients signified by $U_N$ in a NOMA framework.
The power allocated to a client relies on the forces of different clients, because of the BS all out force requirement, $P_t = \sum_{n=1}^{N} P_n^d$, where $P_t$ is the absolute BS power. The signal received by the $n$-th user is termed $y_n = h_n x + w_n$, where $h_n$ indicates the channel gain between the user $n$ and the BS and $w_n$ represents the Gaussian noise at the receiver for user $n$ [23], [24].
Downlink NOMA utilizes a power allocation mechanism, where high power transmission is utilized for clients with below-par channel conditions and vice versa. Accordingly, at a given client in the NOMA group, the strong interfering signals are caused primarily by the powerful message signals of generally frail channel clients. In that capacity, in order to separate the ideal signal, every client cancels the strong interference by SIC translating, demodulating, and by deducting them from the received signal $y$. Consequently, the highest channel gain client drops all intra-cluster interferences, while the least channel picks up a client gets the interferences from all clients within its group [25], [26]. Additionally, the transmitting power is subject to [27]:

$$\sum_{n=1}^{N} P_n^d \leqslant P \ . \tag{1}$$

We expect that the signal received by every client $U_N$ is parted into two streams, and the power fraction with condition $0 \leqslant \theta_n \leqslant 1$ is utilized for data processing. Transmitters are the source of interference $I$. There is a simultaneous transmission of data signals and power from BS. The perception at the $n$-th client, which is utilized for data interpreting, is given by:

$$y_n = h_n \sqrt{\theta_n} \sum_{i=1}^{N} \sqrt{P_i^d} s_i^d + \sqrt{\theta_n I_n} + w_n \ , \tag{2}$$

where $w_n$ indicates additive noise at $U_n$ and $I_n$ is the interfering signal. Noise is included in two parts of the recipient: the receiver antenna noise and the circuit noise. In any case, the antenna noise is ignored. Hence, we incorporate only one additive noise. Each client $U_j$ completes SIC by identifying and eliminating the $U_N's$ message, for all $n < j$, from its perception. Consequently, the attainable rate at $U_N$, $n \in [1, 2, \ldots, N]$ is limited by:

$$R_n^d = \min(R_{n\to n}^d, R_{n\to n+1}, \ldots, R_{n\to N}^d) \ . \tag{3}$$

$R_{n\to j}^d$ indicates the amount at which user $U_j$ finds the intended message for user $U_N$:

$$R_{n\to j}^d = \tau \log_2 \left(1 + \frac{P_n^d \theta_j g_j}{\theta_j g_j \sum_{i=n+1}^N P_i^d + \theta_j P_I, j+1}\right) \ , \tag{4}$$

where $P_n^d = \frac{P_n^d}{N_0}$ and $P_{I,j} = \frac{P_{I,j}}{N_0}$ are the interference power received by $U_j$. We consider that $P_{I,j}$ is detected precisely by $U_j$ and portrayed to the BS to guarantee and allocate the current resources. When $n = N$, Eq. (4) is:

$$R_{n\to j}^d = \log_2 \left(1 + \frac{P_n^d \theta_N g_n}{\theta_N P_{I,N} + 1}\right) \ . \tag{5}$$

$P = P_1^d, \ldots, P_N^d$ shows the set of the power transmission values between the clients and $\theta = \theta_1, \ldots, \theta_N$ is the set of isolating power factors between the clients.

### *4.2. Uplink NOMA*

In uplink NOMA, each client transmits its individual signal $x_n^u$ with:

$$x = \sum_{n=1}^N \sqrt{P_n^u} x_n^u$$

and transmit power $P_n^u$ in such a way that the BS received signal can be characterized as:

$$y = \sum_{n=1}^M \sqrt{P_n^u} h_n x_n^u + w \ ,$$

where $w$ is the receiver noise (with a density of power spectral $N_0$) at the BS. The power transmitted per client is restricted by the client's maximum battery power [23].

Note that, for applying SIC and decrypting signals at the BS, it is essential to keep up the uniqueness of different message signals which are superimposed within $y$. Considering that the channels of various clients are diverse in the uplink, individual message signals encounter definite channel gains. Subsequently, the received signal power, compared with the most potent channel client, is likely the most potent at the BS. Accordingly, this signal is decrypted, first at the BS, and encounters interference from all clients in the group with generally more vulnerable channels. Hence, the communication of the most potent channel gain client encounters interference from all clients within its group, though the communication of the least channel gain client receives zero interference from the clients in its group. In this way, the perception at the BS is given by [27]:

$$y = \sum_{n=1}^N \bar{h}_n \sqrt{P_n^u s_n^u} + I + v \tag{6}$$

where $I$ indicates the interfering signal and $v$ is the additive noise at the BS. By utilizing SIC, the capacity region is limited by:

$$\sum_{n\in M_k} R_n^u \leqslant (1-\tau) \log_2 \left(1 + \frac{\sum_{n\in M_k} P_n^u g_n}{P_I + 1}\right) \forall \, M_k : M_k \subseteq N \ , \tag{7}$$

with $R_n^u$ being a quantum of UL accomplished by the $n$-th client, $P_n^u = \frac{P_n^u}{N_0}$, $P_1 = \frac{P_1}{N_0}$, $N_0$ is the noise power, and $P_I$ is the interference power acquired by the BS. $P_I$ is detected precisely by the BS. At last, $M_k$ signifies any conceivable subset of the clients. $\tau$ is introduced to denote the effect of cross-correlation. The asymptotic Shannon capacities on the UL ($C_{UL}$) and the DL ($C_{DL}$) for MU-MIMO channels under convenient transmission are given by [21]:

$$C_{UL} = \sum_{n=1}^N \log_2(1 + \gamma_n^u M \beta \psi_n) \ , \tag{8}$$

$$C_{DL} = \max_{a_n \geqslant 0, \sum a_n \leqslant 1} \sum_{n=1}^N \log_2(1 + \gamma_n^d M a_n \psi_n) \ , \tag{9}$$

where $\gamma_n^u$ and $\gamma_n^d$ are the overall UL and DL SNR's, $[\psi_n], n = 1, 2, \ldots, N$ constitutes the coefficients of large-scale fading for the $N$ UE's, and $a_n$ is a group of variables which should be enhanced to get $C_{DL}$. At the point when suitable power control systems are utilized to standardize the impact of $\beta_n$, the UL capacity improves to $N \log_2(1 + M\gamma_n^{uSNR})$.

Corresponding considerations are given to DL NOMA. Hence, we accomplish multiplexing gains and cluster gains, under suitable transmission conditions, utilizing simple linear processing techniques at the BS, such as, for example, maximal ratio combining (MRC) and zero forcing (ZF) detection. This streamlines the computational burden and the hardware requirements related to the BSs, the BS's actualize complex signal processing techniques, for example, maximum likelihood (ML) recognition and successive interference cancelation (SIC), to accomplish optimal capacities.

The sum power utilization $P$, accumulated across UL and DL transmissions in a NOMA-MIMO framework, can be displayed as [21]:

$$P = P_{PA} + P_C + P_{sys} \ , \tag{10}$$

where $P_{PA}$ shows the complete DL and UL used through the power amplifiers (PA's) at the UEs and the BS, $P_C$ constitutes the absolute DL and UL circuit power utilized by different digital and analog signal processing circuits at the BS and the UEs and $P_{sys}$ refers to the excess framework-dependent component in $P$.

While $P_{PA}$ empowers for the sum power use on RF transmissions, $P_C$ incorporates the sum power utilization from

RF chain components, for example, synthesizers and filters, additionally the tasks of the baseband, for example, digital up/down conversion, FFT/IFFT, recipient/precoding combining, channel deciphering/coding, and assessment of the channel. Here, $P_C$ can not be planned according to the regular exercise as a stable term autonomous of $(M,K)$ as per the requirement of hardware and the number of circuit processes in the framework created with $K$ and $M$. $P_{sys}$ will assume a critical role in describing energy efficiency of 5G networks, since many BS and UE types will co-exist in a multi-tier architecture with various cell sizes, power utilization levels and access technologies.

### *4.3. Full-Duplex-NOMA System*

We consider a full duplex multicarrier NOMA (FD MC-NOMA) framework which includes full duplex base stations (FD-BSs), $K$ DL clients, and $J$ UL clients. All DL and UL clients are provided with two antennas. The FD-BSs are additionally furnished with two antennas for facilitating synchronized DL transmission and UL reception in a similar frequency band. We expect that the BSs and the DL clients are furnished along with successive interference cancelers. The whole frequency $W$ band is apportioned into $N_F$ subcarriers. In this article, the individual subcarriers are distributed between two DL clients and two UL clients at the most, to restrict multi-user interference (MUI) and the UL-to-DL co-channel interference (CCI) on an individual subcarrier and to guarantee low hardware complexity and low processing delays [28], [29].

Presuming that UL clients $r \in (1,\ldots,J)$, UL clients $t \in (1\ldots.,J)$, DL clients $m \in (1,\ldots,K)$ and DL clients $n \in (1,\ldots,K)$ are preferred and multiplexed on subcarrier $i \in (1,\ldots,N_B)$ likewise the required signals at DL client $n$, DL client $m$, and the BS are indicated likewise by:

$$Y^i_{DL_m} = \sqrt{P^i_m \beta_m} h^i_m x^i_{DL_m} + I^i_{MU_m} + I^i_{CC_m} + w^i_{DL_m} \ , \quad (11)$$

$$Y^i_{DL_n} = \sqrt{q^i_n \beta_n} h^i_n x^i_{DL_n} + I^i_{MU_n} + I^i_{CC_n} + w^i_{DL_n} \ , \quad (12)$$

$$Y^i_{BS} = \sqrt{q^i_r \bar{\omega}_r} g^i_r x^i_{UL_r} + \sqrt{q^i_t \bar{\omega}_t} g^i_t x^i_{UL_t} + I^i_{SI} + w^i_{BS} \ , \quad (13)$$

where $x^i_{UL_r}$ and $x^i_{DL_m}$ represent the transmission of signals from UL client $r$ to the FD-BS and from the FD-BS to DL client $m$ on subcarrier $i$. $P^i_m$ and $q^i_r$ are transmit powers of DL client $m$ and UL BS $r$, separately. $\beta_m$ and $\beta_n$ are the joint impact of path loss and shadowing among DL clients and UL BS. $h^i_r$ and $h^i_m$ indicate the small scale fading coefficients for the link between UL BS $r$ and the FD-BS and the link between the FD-BS and DL client $m$. $I^i_{MU_m}$ and $I^i_{CC_m}$ are MUI and CCI. The joint impact of path loss and shadowing between UL BS $r$ and the FD BS and between DL client $m$ and UL BS $r$ is depicted by $\bar{\omega}_r$ and $g_r$. Finally, the complex additive white Gaussian noise (AWGN) on subcarrier $i$ is depicted by $w^i_{DL_m}$, $w^i_{UL_r}$, and $w^i_{BS}$.

An instant subcarrier is assigned to the clients of two DL and UL in the FD MC-NOMA framework simultaneously. Commonly, the UL power of client signals is lower than that of signals released by the BS for DL clients, which makes it complex for the clients of DL to extract and remove the UL signal by accomplishing SIC. Because of their various constraints on the complexity of receiver hardware and QoS needs, different coding schemes and modulations are used in the DL and UL. As a result, DL clients cannot decode and demodulate the UL signals. So, every user signal is treated as noise, and to eliminate other DL clients, only the DL client achieves SIC. For example, we initially consider an individual policy for the SIC decoding order 4 and an allocation of subcarrier. UL BSs $r$, $t$ and DL clients $m$, $n$ are multiplexed on subcarrier $i$. In addition to decoding SIC and eliminating the DL client, $ms$ signal is achieved by the DL client $n$. Before decrypting the UL client $ts$ signal, the FD BS first decrypts the UL client $rs$ signal and then eliminates it by SIC. Equation (14) is applied to represent the weighted sum throughput of subcarrier $i$ in such an approach:

$$U^i_{m,n,r,t} = s^i_{m,n,r,t} \Bigg[ w_m \log_2 \left(1 + \frac{H^i_m P^i_m}{\alpha^i_m + 1}\right) + w_n \log 2 \left(1 + \frac{H^i_n P^i_n}{\alpha^i_n + 1}\right) + \mu_r \log_2 \left(1 + \frac{G^i_r q^i_r}{\phi I_s I^i \alpha^i_r + 1}\right) + \mu_t \log_2 \left(1 + \frac{G^i_t q^i_t}{\phi I_s I^i \alpha^i_t + 1}\right) \Bigg] \ , \quad (14)$$

for the links between the DL, clients $m$ and $n$ and FD BSs $r$ and $t$ on subcarrier $i$ are defined by the total small scale fading coefficients, such as $\alpha^i_m$, $\alpha^i_n$, $\alpha^i_r$ and $\alpha^i_t$ respectively. The subcarrier allocation indicator is represented by $s^i_{m,n,r,t} \in (0,1)$. If UL BSs $t$ and $r$ and DL clients $n$ and $m$ are multiplexed on subcarrier $i$, then $s^i_{m,n,r,t} = 1$. Before decrypting the BS $ts$ signal, the FD BS first decrypts UL BS $rs$ signal and eliminates it. Likewise, DL client $n$ executes SIC of the DL client $m$ signal. Another resource allocation policy is utilized when $s^i_{m,n,r,t} = 0$. To achieve a particular notation of fairness in resource allocation, the non-negative constants that are identified in the media access control (MAC) layer and $0 \le w_m \le 1$ and $0 \le \mu_r \le 1$ Eq. (14) mentions the preferences of DL client $m$ and UL BS $r$ respectively.

In practice, self-interference (SI) cannot be canceled completely, regardless of whether the SI channel is known at the FD-BS, because of the limited dynamic range of the receiver. Subsequently, we mold the surplus SI following elimination at the receiving antenna with autonomous zero-mean Gaussian distortion noise, for which change is relative to the received power of the antenna. NOMA frameworks utilize the power domain for multiple access, wherein various clients are provided with various power levels. Specifically, for a particular subcarrier, let us presume that the DL client $n$ intends to decrypt and eliminate the CCI induced by DL client $m$ employing SIC. Interference cancelation is fruitful if SINR received by client $ns$ for client $m$ signal is bigger than or equivalent to the SINR received received by client $m$ for its signal. For instance, DL client $n$ can only successfully decrypt and eliminate DL client $m$ signal

by SIC on subcarrier $i$ when the accompanying disparity holds:

$$w_n \log_2\left(1+\frac{H_n^i P_n^i}{\alpha_n^i+1}\right) \geqslant w_m \log_2\left(1+\frac{H_m^i P_m^i}{\alpha_m^i+1}\right) , \quad (15)$$

on subcarrier $i$, the suddenly weighted sum throughput Eq. (14) for the instance of $r=t$ and $m=n$, turn out to be:

$$U_{m,n,r,t}^i = s_{m,n,r,t}^i \Big[ w_m \log_2(1+\frac{H_m^i(P_m^i+P_n^i)}{\alpha_m^i+1}) + \mu_r \log_2\left(1+\frac{G_r^t(q_r^t+q_t^i)}{\phi I_s I^i(\alpha_r^i+1)}\right)\Big] . \quad (16)$$

Variable $\phi$ denotes path loss exponent, $\mu$ is the non-negative constant, the constant parameters $H$ and $G$ are defined as $H_m^i = \frac{\varpi_m |h_m^i|^2}{\sigma_{zDL_m}^2}$, $G_r^i = \frac{e_r |g_r^i|^2}{\sigma_{zBS}^2}$ in Eqs. (14)–(16). The joint UL/DL NOMA channel allocation issue is that, allocating a path for a node either a BS or end client among various nodes in a wireless mesh network, to reduce the processing time and to expand the framework throughput. In our definition, the correspondence between nodes in the backhaul network in a 5G framework can be preoccupied as TSP.

Here, we consider a well-known TSP, in which we need to determine the shortest closed path between clients of both $J$ UL and $K$ DL, with at least one subcarrier allocated to each client. Suppose, $i=(1,2,\ldots,N)$ is the set of TSP clients and the weighted sum throughput of each client is given by $U_{m,n,r,t}^i$.

The system aims to increase the weighted sum throughput of the system. The best joint UL/DL NOMA distribution policy is obtained by mixed-integer linear programming, problem for TSP is represented as:

$$Q(x) = \text{maximize}_{p,q} \sum_{i=1}^{N_F}\sum_{m=1}^{K}\sum_{n=1}^{K}\sum_{r=1}^{J}\sum_{t=1}^{J} U_{m,n,r,t}^i , \quad (17)$$

subject to:

$$C1 : s_{m,n,r,t}^i \in [0,1], \forall_{i,m,n,r,t} , \quad (18)$$

$$C2 : \sum_{i=1}^{N_F}\sum_{m=1}^{K}\sum_{n=1}^{K}\sum_{r=1}^{J}\sum_{t=1}^{J} s_{m,n,r,t}^i (P_m^i+P_n^i) \leqslant P_{max}^{DL} , \quad (19)$$

$$C3 : \sum_{i=1}^{N_F}\sum_{m=1}^{K}\sum_{n=1}^{K}\sum_{r=1}^{J}\sum_{t=1}^{J} s_{m,n,r,t}^i (P_r^i+P_t^i) \leqslant P_{max}^{UL} , \quad (20)$$

$$C4 : \sum_{i=1}^{N_F}\sum_{m=1}^{K}\sum_{n=1}^{K}\sum_{r=1}^{J}\sum_{t=1}^{J} s_{m,n,r,t}^i \leqslant 1, \ \forall i , \quad (21)$$

$$C5 : P_m^i \geqslant 0, \ \forall \ i,m , \quad (22)$$

$$C6 : P_r^i \geqslant 0, \ \forall \ i,r . \quad (23)$$

If $s_{m,n,r,t}^i = (0,1)$, then C1 assures effective SIC at DL operator $n$. For the reception of UL, since the receiver for all UL signals is the FD-BS, it can accomplish SIC in any order. For the BS, the C2 constraint is the power constraint through an extreme allowance of power transmission $P_{max}^{DL}$. By using $P_{max}^{UL}$, C3 bounds the transfer power of UL user $r$. To guarantee that each subcarrier constraint C4 is imposed, it is allocated to the top two DL and UL clients. The client pairings of DL, UL-to-DL, and UL are accomplished on each subcarrier. For the UL and DL clients, C5 and C6 are said to be the non-negative power transmission constraints.

### *4.4. Modified Particle Swarm Optimization (MPSO) with Inertia Weight*

Eberhart and Kennedy discovered a particle swarm optimization (PSO) algorithm relying on a population-based, cooperative search metaheuristic procedure. PSO particles are known as the population's candidate solutions in which it coincides and develops instantly according to the sharing of knowledge from neighboring particles. PSO is a modern optimization algorithm, but when the problem dimension arises, it normally requires some enhancements [31].

In this paper, an altered PSO algorithm is proposed. For planning a modern multi-stage exception expansion, MPSO is applied here. Also, for multi-stage planning, some groups of particles are separated from the population in the altered PSO algorithm. Here, $x_{ij}$ represents the position vector of the $j$-th particle of the $i$-th group. An intermediate network is optimized by each group of particles during single stage iterations. Therefore, the number of planning stages and groups tends to be similar. The particles fly sequentially from dissimilar groups (i.e. dissimilar phases). From its own last position, a $j$-th particle of the first group starts to move in every single iteration, but for $i>1$, from the last position of a $j$-th particle of $i-1$ group, the $j$-th particle of the $i$-th group starts to move. Equation 16 is used to calculate the objective function of each particle for the $i$-th stage in the $i$-th group. The objective function $U_{m,n,r,t}^i$ (where $s=i$) is presented $x_i^{LB}$ as a local best position and it is minimized by the better position vector of the $i$-th group. The overall explanations are gained from the positions of sequential particles of all groups. The number of particles of each group is equal to the number of newly created particles for every iteration.

Equation (17) is used to compute the objective function of every particle. Then, the better solution is predicted. The best particles are presented $x_i^{GB}$ as a better global position. The velocity vector of a better existing position in conventional PSO is calculated as:

$$v_{i,n+1} = w * v_{i,n} + C1 * rd_1(P_{i,n} - x_{i,n}^{LB}) + C2 * rd_2(P_{i,n} - x_{i,n}^{GB}) , \quad (24)$$

$$v_{i,n} = \begin{bmatrix} (1-\frac{t}{T})V_m ; & \text{if } v_{i,n} > V_m \\ -(1-\frac{t}{T})V_m ; & \text{if } v_{i,n} < -V_m \end{bmatrix} , \quad (25)$$

$$x_{i,n+1} = x_{i,n} + v_{i,n+1} . \quad (26)$$

Apart from the scaling term $1-\frac{t}{T}$, an altered algorithm of PSO is almost similar to the original one in the scheme; and in Eq. (25) it is multiplied with maximum velocity $V_m$. The proceeded maximum number of generations processed is

mentioned using $T$ and the number of the current generation is symbolized using $t$.

A significant component inertia weight in particle swarm is used to overcome the local optimal problem and slow rate of convergence of PSO. Inertia weight is one of the important factors to influence the convergence speed and searching for outcomes. The global search ability is better for PSO and when the weight of inertia is higher, then the function of the concrete value is to improve the rate of convergence. Local search ability is also enhanced when the inertia weight is insignificant. This means that an enhanced solution may be achieved immediately after the local search algorithm is completed. Early convergence is processed quickly by the PSO algorithm as well. In the PSO algorithm, we initially fixed a large inertia weight value and in the global scope, to guess the series of the optimum value. To perform the optimal value search for the algorithm, we set a lower value of inertia weight $w$, so that the algorithm offers faster convergence and better search outcomes. The function of the modified inertia weight is:

$$w(x) = \frac{n.\alpha}{n+x^a} + \beta \ , \tag{27}$$

where the rate of change and acceleration factor is defined by $a$, the range of $w$ is controlled by the threshold values (positive constant parameters) $\alpha$ and $\beta$, the current iteration number and the algorithm iteration number are defined by $x$ and $n$, respectively.

The following equations are used to verify the validity of this function:

$$w(x)' = \frac{-n\alpha a x^{a-1}}{(n+x^a)^2} \ , \tag{28}$$

$$w(x)'' = \frac{n\alpha a x^{\gamma-2}(n+x^a)[(a+1)x^a-(a-1)n]}{(n+x^a)^4} \ . \tag{29}$$

When $x$ is greater than $\sqrt{\frac{(\gamma-1)n}{\gamma+1}}$ then the significance of $w(x)''$ is in excess of 0 and $w(x)'$ is lower than 0 as per Eqs. (28) and (29).

The weight of the inertia function is a convex, as well as descending function besides it, is observed from the above formula that the descending speed steadily slows down when the iteration number increases. Without affecting the precision of convergence, it significantly raises the rate of convergence of this algorithm.

The values of $\alpha$ and $\beta$ are set to 0.8 and 0.5, because the range of inertia weight $w$ ranges from 0.5 to 1.2 in PSO. In an existing space, searching for the smaller value of w takes place but the bigger w can be searched in the new spaces. The inertia weight variable is suitably picked for balancing both the local and global search. In Eq. (27), a different value of $a$ is displayed for the inertia weight function.

In the process of its execution, the algorithm preserves two superior variables named g-best and l-best position. Two comparisons are performed: to decide the g-best location of every creation in the entire population, each particle's fitness at its current position is related to the remaining particles' fitness. Then, to choose the l-best position for every particle, the current location of separate particles is contrasted with diverse visiting positions. Based on Eq. (24), the refining velocity of every particle in the species of particle group is realized by these two positions. To update the speed rate of the fresh particle, two stochastic variables outweigh the effect of two locations.

The pseudo-code with the M-PSO algorithm for task scheduling is presented as Algorithm 1.

**Algorithm 1. Modified PSO for joint UL/DL channel allocation**

1. **Initialization**. The population and iteration number are fixed as $N$ and $N_t$, respectively. Within the predefined decision variable range, initialize velocity $v_i$ and position $x_i$ of the particles with random numbers. The upper bound of the decision variable is fixed at $V_m$. The fixed iteration count $t = 0$ and $p_i = x_i$ as personal better position.

2. **Estimation**. Every single particle in the current population is estimated. Set $t = t+1$, $p_i = x_i$ when $Q(t) < Q(t-1)$. Find a corresponding position $x_{\min}$ and $Q_{\min} = \min Q(t)$. The global best is selected by using $x_{i,n}^{GB} = x_{\min}$.

3. **Generation of new particles**. Compute the objective function values for every single new particle and, depending upon the current $x_i$ ($i = 1, 2, \ldots, N$), compute the new position $x_i$ and velocity $v_i$. Associate new $x_i$ ($2N$ particles) as well as all $x_i$ together and collect them in a temporary list.

4. **Non-dominated sorting**. In *tempList* recognize dominated results and save them in a $P_{front}$ (Pareto front) matrix. Fixed front number $k = 1$ and:

   (a) from the *tempList* the non-dominated particles are eliminated,

   (b) $k = k+1$. The non-dominated results in the excepting *tempList* are recognized and are collected in a $P_{front}k$ (front $k$) matrix,

   (c) when all $2N$ particles get ranked into several fronts then stop the repeating steps b–c.

5. **For the next iteration, select particles**. From $P_{front}$ randomly pick out $N$ particles, if $P_{front}size > N$ and store them as next $x_i$. Or select random particles in next front (front $k$) and include them in next $x_i$ until next $x_i$ size becomes $N$.

6. For every particle in next $x_i$, compute objective function values and for the next iteration set the next $x_i$ as the current position's $x_i$.

7. If all $v_i < 0.1V_m$, then implement subsequent steps or else go to step 8.

   (a) from the current population randomly pick 20% particles and modify their positions by 10% of

the $V_m$. Finally, $x_{temp}$ is used to store those results,

(b) $x_{temp}$ gets estimated and all the dominant particles are identified. The particles in the current $x_i$ are replaced by those dominating particles,

(c) it is definite that the number of $x$ does not exceed $N$ and repeat $K$ times ($K = 1, 2, \ldots, 10$) steps a–b.

8. If $t < N_t$ go to step 2.

9. From the final population, the non-dominated solutions are stored and performance metric values are calculated.

The creation of randomized and legal influence of location is a major goal of these coefficients. So, once in a while it is very essential to find few examinations and at other times small exploitation stochastically. Depends upon a new speed with solving Eq. (26), this algorithm updates the particle's current position to a new value. Every single particle defines the PSO particle population's new state and reviews its position. Based on their new location, the fitness values are evaluated by the algorithm. The duplication of the processes is used to estimate the location of fresh particles and to predict the global and the local best positions which, in turn, are used to inform the position of the particles.

Table 2
Simulation parameters

| Parameter | Description |
|---|---|
| System bandwidth | 12 GHz |
| Number of subcarriers | 5 |
| Carrier frequency | 3.6 GHz |
| Subcarrier separation | 20 kHz |
| Sub-frame length | 1.0 ms |
| Symbol duration | 66.67 $\mu$s + cyclic prefix: 4.69 $\mu$s |
| Receiver type | MMSE+SIC |
| Number of users per cell | 10 |
| Number of PU per cell | 3 |
| Number of SU per cell | 7 |
| Inter-site distance | 500 m |
| Maximum transmit power | 46 dBm |
| Channel model | 3GPP spatial channel model (SCM) |
| Path loss model | $133.6 + 35 \log(d)$ [km] |
| Traffic model | Full buffer |
| Power factor | 0.25 |
| Size of swarm | 30 |
| Modulation technique | 16 QAM |
| Maximum iteration | 500 |
| Encoding | Conventional |

# 5. Performance Evaluation

The performance of the presented channel allocation method is examined using the simulation parameters from Table 2. Within the outer and inner boundaries, both the $K$ and $J$ users are uniformly and randomly dispensed. $P_{max}^{DL}$ defines the extreme transmit power of the FD BS. Here, we incorporate the Rayleigh fading model in the UL NOMA for communication between users and the BS. Similarly, we have incorporated the Rician fading model in the DL NOMA for communication between the BS and users.

## *5.1. Throughput*

Throughput is defined as the movement of data from one location to another, over a specific period of time. It is a key indicator of the effectiveness and quality of network connectivity. A high rate of failed message deliveries will eventually lead to low throughput and degraded performance. Decoding methods in NOMA systems, to decode various simultaneous transmissions, SIC which is a multiuser detection technique that uses the structured nature of interference. Separate signals are retrieved, one by one, from the composite signal in the following manner. It is questionable when the remaining signals are decoded if all of the signals fail to be decoded. Throughput depends on every single signal. The order of decoding also plays an essential role in the positive outcome of decoding operation. The order of decoding the received superposition coded signals is not forced by the principle of NOMA. The system's advantages become visible when throughput decodes stronger signals ahead of their weaker counterparts.

However, due to the decoding difficulties of the SIC method and the changing nature of wireless channels, most users are allocated, undesirably, to subchannels which will intensify the system's throughput. Throughput of the presented system increases with the increasing number of users, as shown in Fig. 2 and is compared with some of the existing approaches [25].

Consistent throughput performance was obtained in the graph for the existing algorithms, where the number of users does not affect throughput to a considerable degree. Tree search-based transmission power allocation (TTPA) and fractional transmission power allocation (FTPA) are the conventional methods that work based on grouping, power allocation, and ordering. Figure 2 shows that the proposed system is affected by significant changes concerning the number of users. Typically, NOMA systems are intended for dense user networks. The proposed system is highly suitable here. Extreme throughput is achieved by users who gain the best of all subchannels. Similarly, the maximum throughput is achieved by the users who are nearer to the base station, as well as in overall subchannels, with the effect of Rayleigh fading being statistically parallel for all users.

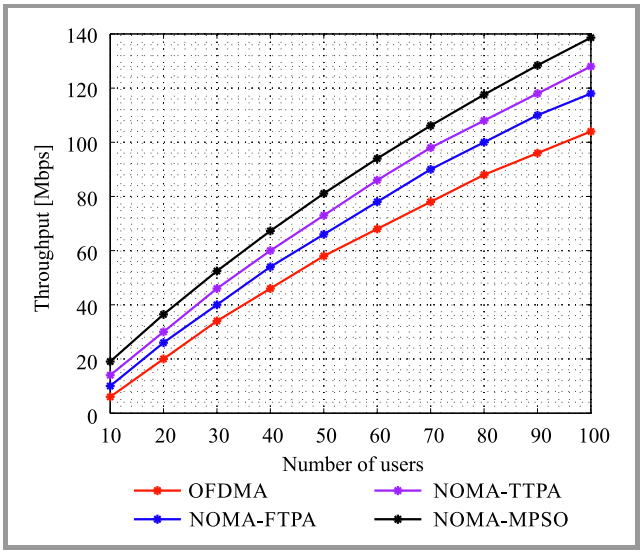


*Fig. 2.* Throughput vs. number of users.

### 5.2. Spectral Efficiency

Spectral efficiency is defined as the bits per second net data rate divided by bandwidth. Net data rate and index rate are associated with the raw data rate, including the payload and all overheads that can be used. Figure 3 shows the spectral efficiency versus the number of users. The NOMA-MPSO spectral efficiency exceeds the NOMA-TTPA, NOMA-FTPA, and OFDMA schemes and the presented methods of resource optimization tend to provide maximum spectral efficiency than the existing previous techniques [32], [33].

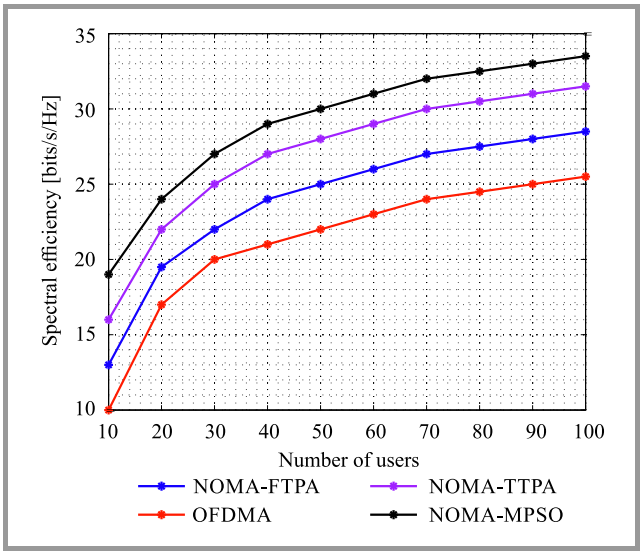


*Fig. 3.* Spectral efficiency vs. number of users.

Figure 3 shows that with the number of users, the efficiency of the spectrum rises and the growth of data rate becomes slower with the rise in the number of users. It endures rising in the total sum rate when the number of users is greater than the number of sub-channels as well as it grows at a smaller speed due to the gain of multiuser diversity. When the user number is insignificant then the effect of diversity of multiuser is more remarkable.

### 5.3. Sum-Rate

The sum rate is defined as the sum of all rates of communication between the nodes, taking place in a network:

$$R_T = \sum_{k=1}^{K} R_k \ , \tag{30}$$

where $R_k$ is the $k$-th user equivalent sum-rate and $R_T$ is the sum-rate obtained by using the proposed approach. The highest sum-rate for users will be achieved by conducting all communication at once, or there must be some scheduling between the different tasks. The sum-rate is maximized when the system is operating continuously, in the full-duplex mode.

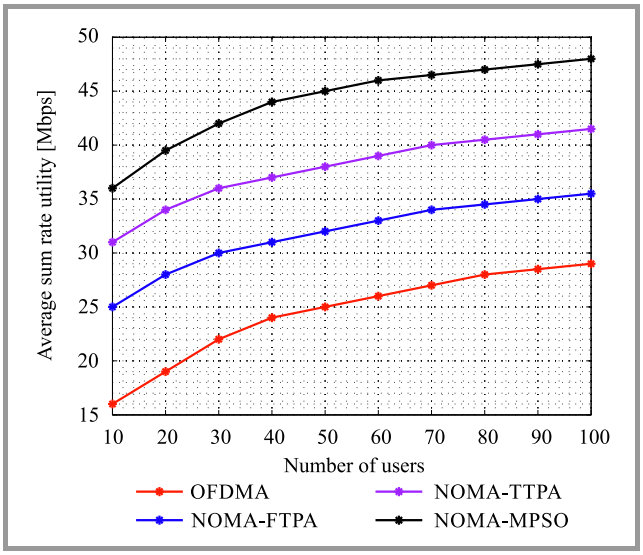


*Fig. 4.* Sum rate vs. number of users.

Figure 4 shows $R_T$, the total rate of the user, the number of UEs per cell function, is got through system-level simulations for the presented scheme of NOMA-MIMO using MPSO at the SIC receiver at both ends and transmitter side of BS. We put in a simple assessment model using the Shannon capacity [34]. Using NOMA, we assess a case accounting OFDMA, in which the transmission of a single-stream is applied per transmitter beam. In addition, MPSO channel allocation methods are compared with the exhaustive NOMA-FTPA and NOMA-TTPA searches. The NOMA-MPSO technique is suitable for finding the constraints of QoS and the sum-rate with weights in which the majority of the gap is less than 5% and it is very adjacent to the globally optimum value. Hence, the suggested joint UL/DL channel assignment technique is capable of attaining approximate optimal performance with fewer difficulties.

### 5.4. Outage Probability

Outage probability is the achieved data rate of an individual user which is lower than the predefined value. For common outage probability, an outage occurs when the user is deactivated. In individual outage probability, individual user outage events are considered. Outage probability is used as a performance measure, since it not only allows for the identification of the probability of errors, but may be also used to evaluate the outage capacity/rate. After 20 dB, the graph gets saturated due to the proper achievement of SNR in this region. The effect of the user's non-uniform locations and the interference is caught by applying stochastic geometry, and the order of diversity is computed to demonstrate efficient use of the channel's degree of freedom by the presented framework [35]. In Fig. 5, the scheme in question is compared with NOMA-TTPA, NOMA-FTPA, OFDMA. One may notice that their outage sum-rate performance is similar, up to a certain reduced number of users, but when the number of users increases, outage probability changes considerably. However, the NOMA-MPSO scheme is capable of offering much better reception reliability, certainly for maximum power transmissions.

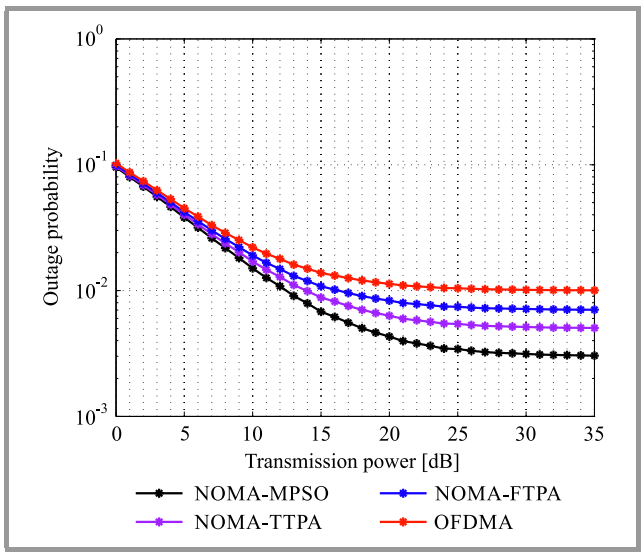


*Fig. 5.* Outage probability vs. transmission power.

### 5.5. SINR

SINR measures the quality of a transmission channel. SINR is generally defined for a specific user and is represented as:

$$SINR = \frac{P}{I+N}\ , \tag{31}$$

where incoming signal, interference signal, and noise are denoted as $P$, $I$, and $N$, respectively. Noise cancelation is impossible under separate constraints of power, but the possibility of the set of target SINRs may be under a sum power constraint. Because of the unavailability of power constraints, arbitrary target SINRs may be achieved. This is caused by the cascaded structure of interference formed by the successive decoding operations. To accomplish a certain set of SINRs, an equal amount of total power is essential for both links. Under a sum power constraint, both links have an equal achievable SINR range. Likewise, the same beamformers, accomplish the target [36]. Figure 6 illustrates the performance of the offered method BER unit and compares its performance with existing algorithms OFDMA, NOMA-FTPA, and NOMA-TTPA. BER performance is improved in the proposed system.

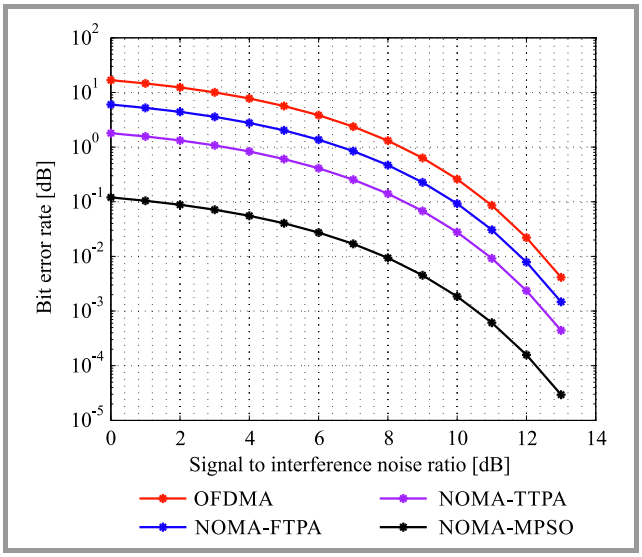


*Fig. 6.* BER vs. SINR.

### 5.6. Fairness

This is the most popular metric used in network engineering to determine if users or applications receive a fair share of he system's resources. Fairness is defined as:

$$Fairness(r_1, r_2, \ldots, r_n) = \frac{(\sum_i r_i)2}{n\sum_i r_i 2}\ , \tag{32}$$

where the throughput individual nodes is denoted as $r_1, r_2, \ldots, r_n$. Based on the scheduling period, the fairness of the proposed method is examined. The time domain of the scheduling process is slotted. The time slot index is denoted by $t$. With 20 slots, we interpret a scheduling frame. Channel state information is grouped once per frame. The Jain's fairness index is calculated by $\frac{(\sum_{k=1}^{K} \overline{r_k})2}{K\sum_{k=1}^{K} \overline{r_k}2}$, when the average user's rates are $\overline{r_1}, \ldots, \overline{r_k}$, at the end of the period of schedule. In network communications, this index, developed in [37] and is utilized for user throughput as a measure of fairness value from $\frac{1}{K}$ and 1.0 is reached. Fairer throughput distribution is specified by higher values. This index will drop the index value but doesn't evade a user from being assisted with low throughput (or even zero throughputs) but it will bring down the index value.

The fairness index for the number of users is shown in Fig. 7. Thanks to the higher level of competition between the users, fairness degradation in all schemes is caused by an increase in the number of users [32]. But in the scheme we propose, the slope of the curve is decreasing slightly

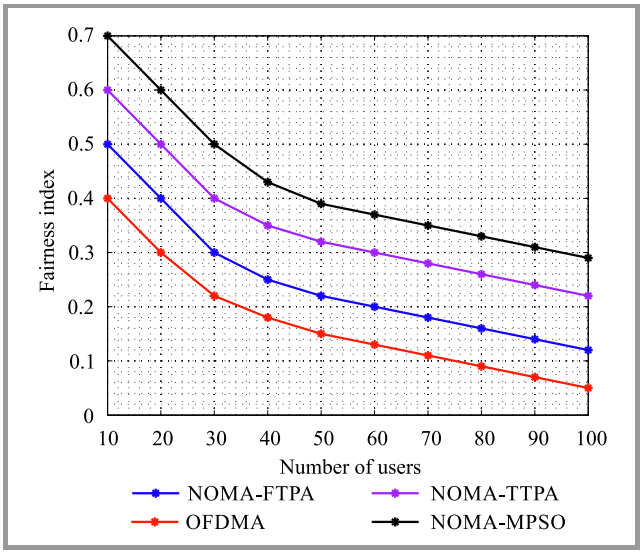


***Fig. 7.*** Fairness index vs. number of users.

with an increase in the number of users, which means that fairness level is improved compared to that of the existing schemes, i.e. OFDMA, NOMA-TTPA, and NOMA- FTPA.

## 6. Conclusion

This paper discusses the design of FD BS for the MIMO-NOMA system channel allocation algorithm. For the enlargement of the weighted sum system throughput, the model of the algorithm is generated as a mixed combinatorial non-convex optimization issue. Based on various workloads and task scheduling approaches, an M-PSO algorithm is developed in this paper. The inner weight factor plays a vital role in M-PSO, where the higher value of inertia weight is performed as global search and the small weight of inertia value performed as local search. The M-PSO algorithm with a greater number of users achieves better results than the same algorithm with a few users. Moreover, the presented FD MC-NOMA approach was proven to offer a perfect balance between maintaining fairness and improving the system's throughput among users. The proposed FD MC-NOMA M-PSO scheme offers better performance in terms of throughput, fairness, sum-rate, and spectral efficiency for a given number of users.

## References

[1] G. A. Akpakwu, B. J. Silva, G. P. Hancke, and A. M. Abu-Mahfouz, "A survey on 5G networks for the Internet of Things: Communication technologies and challenges", *IEEE Access*, vol. 6, pp. 3619–3647, 2018 (DOI: 10.1109/ACCESS.2017.2779844).

[2] A. Boulogeorgos *et al.*, "Wireless terahertz system architectures for networks beyond 5G", *arXiv preprint arXiv:1810.12260*, 2018.

[3] M. A. Khan *et al.*, "Understanding autonomic network management: A look into the past, a solution for the future", *Computer Commun.*, vol. 122, pp. 93–117, 2018 (DOI: 10.1016/j.comcom.2018.01.014).

[4] T. Shuminoski, S. Kitanov, and T. Janevski, "Advanced QoS provisioning and mobile fog computing for 5G", *Wirel. Commun. and Mobi. Comput.*, vol. 2018, article ID 2109394, 2018 (DOI: 10.1155/2018/5109394).

[5] U. Siddique, H. Tabassum, E. Hossain, and D. I. Kim, "Wireless backhauling of 5G small cells: Challenges and solution approaches", *IEEE Wirel. Commun.*, vol. 22, no. 5, pp. 22–31, 2015 (DOI: 10.1109/MWC.2015.7306534).

[6] I. Aldmour, "Wireless broadband tools and their evolution towards 5G networks", *Wirel. Personal Commun.*, vol. 95, no. 4, pp. 4185–4210, 2017 (DOI: 10.1007/s11277-017-4058-x).

[7] S. M. R. Islam, N. Avazov, O. A. Dobre, and K.-S. Kwak, "Power-domain non-orthogonal multiple access (NOMA) in 5G systems: Potentials and challenges", *IEEE Commun. Surveys & Tutor.*, vol. 19, no. 2, pp. 721–742, 2016 (DOI: 10.1109/COMST.2016.2621116).

[8] C. Sexton *et al.*, "5G: Adaptable networks enabled by versatile radio access technologies", *IEEE Commun. Surveys & Tutor.*, vol. 19, no. 2, pp. 688–720, 2017 (DOI: 10.1109/COMST.2017.2652495).

[9] N. Bui *et al.*, "A survey of anticipatory mobile networking: Context-based classification, prediction methodologies, and optimization techniques", *IEEE Commun. Surveys & Tutorials*, vol. 19, no. 3, pp. 1790–1821, 2017 (DOI: 10.1109/COMST.2017.2694140).

[10] T. H. Naveen and G. Vasanth, "Qualitative study of existing research techniques on wireless mesh network", *Int. J. of Adv. Comp. Sci. and Appl.*, vol. 8, no. 3, pp. 49–57, 2017 (DOI:10.14569/IJACSA.2017.080308).

[11] A. BenMimoune and M. Kadoch, "Relay technology for 5G networks and IoT applications", in *Internet of Things: Novel Advances and Envisioned Applications*, D. P. Acharjya and M. K. Geetha, Eds. *Studies in Big Data*, vol. 25, pp. 3–26. Springer, 2017 (DOI: 10.1007/978-3-319-53472-5_1).

[12] E. Ezhilarasan and M. Dinakaran, "A review on mobile technologies: 3G, 4G and 5G", in *Proc. 2nd Int. Conf. on Recent Trends and Challen. in Comput. Models ICRTCCM 2017*, Tindivanam, India, 2017, pp. 369–373 (DOI: 10.1109/ICRTCCM.2017.90).

[13] W. Xia, Y. Zhou, G. Yang, and R. T. Chen, "Power-balanced non-orthogonal multiple access based on virtual channel optimization", *IEEE Trans. on Circ. and Syst. II: Express Briefs*, vol. 67, no. 4, pp. 795–799, 2019 (DOI: 10.1109/TCSII.2019.2925270).

[14] M. Dighriri, G. M. Lee, and T. Baker, "Measurement and classification of smart systems data traffic over 5G mobile networks", in *Technology for Smart Futures*, M. Dastbaz, H. Arabnia, and B. Akhgar, Eds. Springer, 2018, pp. 195–217 (DOI: 10.1007/978-3-319-60137-3_9).

[15] Z. J. Ali, N. K. Noordin, A. Sali, and F. Hashim, "Fair energy-efficient resource allocation for downlink NOMA heterogeneous networks", *IEEE Access*, vol. 8, pp. 200129–200145, 2020 (DOI: 10.1109/ACCESS.2020.3035212).

[16] I. Ahmad, Z. Kaleem, R. Narmeen, L. D. Nguyen, and D.-B. Ha, "Quality-of-service aware game theory-based uplink power control for 5G heterogeneous networks", *Mob. Netw. and Appl.*, vol. 24, no. 2, pp. 556–563, 2019 (DOI: 10.1007/s11036-018-1156-2).

[17] S. Han, X. Xu, X. Tao, and P. Zhang, "Joint power and sub-channel allocation for secure transmission in NOMA-based mMTC networks", *IEEE Syst. J.*, vol. 13, no. 3, pp. 2476–2487, 2019 (DOI: 10.1109/JSYST.2018.2890039).

[18] Y. Shi, J. Zhang, W. Chen, and K. B. Letaief, "Generalized sparse and low-rank optimization for ultra-dense networks", *IEEE Commun. Magazine*, vol. 56, no. 6, pp. 42–48, 2018 (DOI: 10.1109/MCOM.2018.1700472).

[19] N. U. Hasan *et al.*, "Network selection and channel allocation for spectrum sharing in 5G heterogeneous networks", *IEEE Access*, vol. 4, pp. 980–992, 2016 (DOI: 10.1109/ACCESS.2016.2533394).

[20] X. Gao, O. Edfors, J. Liu, and F. Tufvesson, "Antenna selection in measured massive MIMO channels using convex optimization", in *Proc. IEEE Globecom Worksh. GC Wkshps 2013*, Atlanta, GA, USA, 2013, pp. 129–134 (DOI: 10.1109/GLOCOMW.2013.6824974).

[21] K. N. R. S. V. Prasad, E. Hossain, and V. K. Bhargava, "Energy efficiency in massive MIMO-based 5G networks: Opportunities and challenges", *IEEE Wirel. Commun.*, vol. 24, no. 3, pp. 86–94, 2017 (DOI: 10.1109/MWC.2016.1500374WC).

[22] M. Hadi and R. Ghazizadeh, "Sub-channel assignment and power allocation in OFDMA-NOMA based heterogeneous cellular networks", *AEU – Int. J. of Electron. and Commun.*, vol. 120, article 153195, 2020 (DOI: 10.1016/j.aeue.2020.153195).

[23] H. Tabassum *et al.*, "Non-orthogonal multiple access (NOMA) in cellular uplink and downlink: Challenges and enabling techniques", arXiv preprint arXiv:1608.05783, 2016.

[24] J. Zhu, J. Wang, Y. Huang, S. He, X. You, and L. Yang, "On optimal power allocation for downlink non-orthogonal multiple access systems", *IEEE J. on Selec. Areas in Commun.*, vol. 35, no. 12, pp. 2744–2757, 2017 (DOI: 10.1109/JSAC.2017.2725618).

[25] Y. Saito *et al.*, "Non-orthogonal multiple access (NOMA) for cellular future radio access", in *Proc. IEEE 77th Veh. Technol. Conf. VTC Spring 2013*, Dresden, Germany, 2013 (DOI: 10.1109/VTCSpring.2013.6692652).

[26] A. Benjebbour, K. Saito, A. Li, Y. Kishiyama, and T. Nakamura, "Non-orthogonal multiple access (NOMA): Concept, performance evaluation and experimental trials", in *Proc. Int. Conf. on Wirel. Netw. and Mob. Commun. WINCOM 2015*, Marrakech, Morocco, 2015 (DOI: 10.1109/WINCOM.2015.7381343).

[27] P. D. Diamantoulakis, K. N. Pappi, G. K. Karagiannidis, H. Xing, and A. Nallanathan, "Joint downlink/uplink design for wireless powered networks with interference", *IEEE Access*, vol. 5, pp. 1534–1547, 2017 (DOI: 10.1109/ACCESS.2017.2657801).

[28] Y. Sun, D. K. W. Ng, Z. Ding, and R. Schober, "Optimal joint power and subcarrier allocation for full-duplex multicarrier non-orthogonal multiple access systems", *IEEE Trans. on Commun.*, 65, no. 3, pp. 1077–1091, 2017 (DOI: 10.1109/TCOMM.2017.2650992).

[29] A. Memarinejad, M. Mohammadi, and M. B. Tavakoli, "Full-duplex NOMA cellular networks: Beamforming design and user scheduling", *AEU – Int. J. of Electron. and Commun.*, vol. 126, article 153415, 2020 (DOI:10.1016/j.aeue.2020.153415).

[30] P. S. Shelokar, P. Siarry, V. K. Jayaraman, and B. D. Kulkarni, "Particle swarm and ant colony algorithms hybridized for improved continuous optimization", *Applied Mathem. and Comput.*, vol. 188, no. 1, pp. 129–142, 2007 (DOI: 10.1016/j.amc.2006.09.098).

[31] M. Masdari, F. Salehi, M. Jalali, and M. Bidaki, "A survey of PSO-based scheduling algorithms in cloud computing", *J. of Network and Sys. Manag.*, vol. 25, no. 1, pp. 122–158, 2017 (DOI: 10.1007/s10922-016-9385-9).

[32] B. Di, L. Song, and Y. Li, "Sub-channel assignment, power allocation, and user scheduling for non-orthogonal multiple access networks", *IEEE Trans. on Wirel. Commun.*, vol. 15, no. 11, pp. 7686–7698, 2016 (DOI: 10.1109/TWC.2016.2606100).

[33] M. Jain, S. Soni, N. Sharma, and D. Rawal, "Performance analysis at far and near user in NOMA based system in presence of SIC error", *AEU – Int. J. of Electron. and Commun.*, vol. 114, article 152993, 2020 (DOI: 10.1016/j.aeue.2019.152993).

[34] L. Lei, D. Yuan, C. K. Ho, and S. Sun, "Power and channel allocation for non-orthogonal multiple access in 5G systems: Tractability and computation", *IEEE Trans. on Wirel. Commun.*, vol. 15, no. 12, pp. 8580–8594, 2016 (DOI: 10.1109/TWC.2016.2616310).

[35] Z. Ding, R. Schober, and H, V. Poor, "On the design of MIMO-NOMA downlink and uplink transmission", in *Proc. IEEE Int. Conf. on Commun. ICC 2016*, Kuala Lumpur, Malaysia, 2016 (DOI: 10.1109/ICC.2016.7510759).

[36] M. Aldababsa and O. Kucur, "BER performance of NOMA network with majority based JTRAS scheme in practical impairments", *AEU – Int. J. of Electron. and Commun.*, vol. 129, article 153523, 2021 (DOI: 10.1016/j.aeue.2020.153523).

[37] R. K. Jain *et al.*, "A quantitative measure of fairness and discrimination for resource allocation in shared computer system", Eastern Research Laboratory, Digital Equipment Corporation, Hudson, MA, 1984 [Online]. Available: https://www.cs.wustl.edu/∼jain/papers/ftp/fairness.pdf

**Nirmalkumar S. Benni** is currently an Assistant Professor at the School of Electronics and Communication Engineering, REVA University, Bengaluru, India. He has completed an M.Tech. degree in Digital Communication & Networking, UBDT, Davangere, India in 2007, from Kuvempu University, Shimoga and a B.E. degree in Electronics and Communication Engineering, Hirasugar Institute of Technology, Nidasoshi, Belagavi, India, in 2005, from VTU, Belagavi. He is pursuing his Ph.D. in Electronics and Communication Engineering in the area of wireless communication and networks.
E-mail: nirmalkumar.benni@gmail.com
Department of Electronics and Communication Engineering
REVA Institute of Technology and Management
Rukimini Knowledge Park, Kattigenahalli, SH 104
Srinivasa Nagar, Bangalore
Karnataka 560064, India

**Sunilkumar S. Manvi** received his B.E. degree from Karnataka University in 1987, M.E. degree in Electronics from the University of Visweshwariah College of Engineering, Bangalore, in 1993 and Ph.D. degree in Electrical Communication Engineering, from the Indian Institute of Science, Bangalore, India in 2003. He is currently working as a Principal Investigator at the Wireless Information Systems Research Lab, Principal, REVA Institute of Technology and Management, and a Director of the School of Computing and Information Technology at REVA University. Bangalore, India. His research interests fokus on software agent-based network management, wireless networks, multimedia networking, underwater networks, wireless network security, grid and cloud computing, e-commerce, and mobile computing.
E-mail: ssmanvi@reva.edu.in
Department of Electronics and Communication Engineering
REVA Institute of Technology and Management
Rukimini Knowledge Park, Kattigenahalli, SH 104
Srinivasa Nagar, Bangalore
Karnataka 560064, India